Stability and formation of localized surface waves at the dielectric—photorefractive crystal boundary

Victor Aleshkevich, Yaroslav Kartashov,* and Alexey Egorov

Physics Department, M. V. Lomonosov Moscow State University, Vorobiovy gory, 119899 Moscow, Russia

Victor Vysloukh

Departamento de Fisica y Matematicas, Universidad de las Americas-Pueblo, Sta. Catarina Martir, Codigo Postal 72820, Pueblo, Cholula, Mexico

We consider specific features of the formation of localized surface waves at the interface between linear dielectric and photorefractive crystals with a nonlocal diffusion component of nonlinear response. Profiles of the surface waves are numerically found and guiding properties of the surface are investigated. Stability of the obtained surface waves is considered and it is shown that the well-known Vakhitov-Kolokolov stability criterion derived for the local Kerr or saturable material remains legible for the medium with a nonlocal diffusion component of nonlinear response.

I. INTRODUCTION

Among the classical problems of nonlinear optics is the problem of propagation of the laser beam near the boundary of two media exhibiting different optical properties. The most interesting from the practical point of view is the case of a boundary between nonlinear optical materials. The propagation of the laser beams near the boundaries between Kerr materials (see, for instance, [1–6] for the case of the linear-nonlinear boundary and [7] for the case of the nonlinear-nonlinear boundary), quadratic optical materials [8], as well as propagation at the boundary of the Kerr medium and absorbing medium [9] were already considered in great detail. From a mathematical point of view the problem of interaction of the laser beam with a surface consists of a solution of the equation that belongs to the wide class of nonlinear Schrödinger equations with coefficients, depending on the transverse coordinates. The absence of the translation symmetry in the transverse direction results in this case in the appearance of the structures localized at the boundary between different materials that nevertheless cannot be found with the aid of the methods of the inverse scattering technique even in the case of Kerr nonlinearity.

Starting from the simplest cases of Kerr nonlinear optical materials investigations were carried out to the materials with more complicated nonlinear properties. Recent achievements [10,11] in the generation of optical solitons in photorefractive crystals exhibiting high nonlinear properties at low light intensities have encouraged intense investigations of the photorefractive surface waves. In Ref. [12] specific properties of ''delocalized'' photorefractive surface waves at the boundary between the unbiased photorefractive medium with purely diffusion logarithmic nonlinearity and linear dielectric or an ideal metal were described. Such delocalized surface

waves actually have infinite energy due to the presence of the long slowly decaying oscillating tails going away into the volume of the photorefractive sample (see Ref. [13] for experimental observation of such waves). Formation of the surface wave in this case occurs due the interference between waves reflected from the boundary and Bragg grating formed in the photorefractive sample volume [12]. Later [14,15] stable near-surface localized beam propagation in the presence of both drift and diffusion photorefractive nonlinearity (in the limit of a high dark irradiance level) was interpreted as the result of the stable balance between the effect of total internal reflection from the less optically dense linear medium and the effect of beam self-bending due to the diffusion component of photorefractive nonlinear response [16–19]. In Ref. [15] an analogy between optical solitons and mechanical particles was used to derive an ordinary differential equation of the second order describing the trajectory of the near-boundary beam propagation.

The transient regime of the near-boundary beam propagation has also gained steady attention [20–22]. It was motivated by the fact that the main feature of any photorefractive devise is slow response time—but in general the response time is inversely proportional to the light intensity. However, the laser beam can be self-channeled along the surface of the photorefractive crystal, thus enhancing the intensity in the narrow surface layer and speeding up the photorefractive response [22]. It was shown [20] that in the transient regime the diffusion component of photorefractive response leads to the strong light-induced scattering known as the fanning effect.

Another intriguing and important issue is the stability of the localized surface waves [2–7]. It was shown in [23] that the generalized Vakhitov-Kolokolov (VK) stability criterion that was initially derived for the solitons in a saturable focusing optical medium for two transverse dimensions [24] provides also the stability of the fundamental modes on arbitrary nonlinear waveguiding of both one and two transverse dimensions, including solitons of local homogeneous material and nonlinear surface waves at the interface be-

*Corresponding author. Email address: azesh@gateway.phys.msu.su

tween two local homogeneous nonlinear materials. The simplicity of the method that enables us to make a conclusion about the stability by reading the corresponding dispersion diagrams (dependencies of the mode energies on the value of propagation constant) without further calculations makes it very attractive and calls for the further extension on the cases of more complicated models. At the present moment VK criterion with corresponding modifications was extended to the surface waves in multilayered optical structures, solitons in quadratic optical materials, solitons in the medium with competing quadratic and cubic nonlinearities, and solitons of the set of incoherently coupled nonlinear Schrödinger equations (for the comprehensive review see Refs. [25–34]). However, stability of the surface waves in the presence of the nonlocal component of the nonlinear response have not been addressed so far.

In the present paper we consider surface waves at the interface between the linear dielectric and photorefractive medium with local drift and nonlocal diffusion components of the nonlinear response for the arbitrary dark irradiance level. We have numerically found profiles of the surface waves, investigate guiding properties of the boundary, and perform the linear stability analysis of the obtained solutions.

II. THEORETICAL MODEL

We consider propagation of the slit laser beam (transverse extent of the beam along the y axis greatly exceeds that along the x axis) in the direction of the longitudinal z axis near the boundary between the linear dielectric and nonlinear photorefractive medium with drift and diffusion components of nonlinear response. It is supposed that the linear dielectric occupies an area $x \geq 0$, whereas the nonlinear photorefractive medium occupies an area $x < 0$. The laser beam is linearly polarized along the x axis. The width of the transition area between the linear and nonlinear media (which is always nonzero in a real experiment) is supposed to be small compared with the characteristic extent of the laser beam in the x direction and does not affect the profiles of the surface waves. As will be shown later, propagation of the laser beam in such a geometry can be described with one shortened wave equation regarding the complex x-dependent amplitude of the light field. Inclusion of the y component of the optical field obviously results in a more complicated set of coupled nonlinear equations for the polarization components of the surface waves and the appearance of a number of new effects affecting, for example the stability of the surface waves (i.e., the appearance of polarization instability) and their properties with respect to interaction with other light beams. Moreover, even the propagation of one-component slit laser beams that are widely used in photorefractives for the verification of new theoretical predictions is affected by the development of modulation instability. In our case such instability will unavoidably result in gradual filamentation of the near-surface laser beam in the transverse y direction because the presence of the diffusion component of the photorefractive response extends the bandwidth of the modulation instability domain up to infinity, so any y-dependent perturbation

with an arbitrary spatial period will grow up exponentially in the propagation process. However, the rate of this process strongly depends on the spatial period of perturbation and quickly decreases with a decrease of the perturbation period.

To describe the propagation of the laser beam in the area of a nonlinear photorefractive medium ($x < 0$) we proceed with consideration of the material response of the medium, which in the two-dimensional case can be described by the following standard system of equations for the internal space-charge field $E_{sc}(x,z,t)$ produced by the photoinduced redistribution of the spatial charge [35]:

$$\frac{\partial n_e}{\partial t} = \frac{\partial n_d^+}{\partial t} - \frac{1}{e}\frac{\partial j}{\partial x},$$

$$\frac{\partial n_d^+}{\partial t} = \sigma(I+I_{\text{dark}})(n_d-n_d^+) - \gamma_r n_e n_d^+,$$

$$j = e\zeta n_e(E_0+E_{sc}) - \zeta k_b T \frac{\partial n_e}{\partial x},$$

$$\frac{\partial E_{sc}}{\partial x} = \frac{4\pi e}{\varepsilon}(n_e+n_a-n_d^+). \tag{1}$$

Here n_e, n_d, n_d^+, and n_a are the concentrations of the free carriers, donors, ionized donors, and acceptors, respectively; j is the charge current; σ is the photoionization cross section; I is the intensity of the light beam; I_{dark} describes the dark irradiance level that can be increased due to the introduction of the incoherent background illumination; γ_r is the pair recombination rate; e and ζ are the charge and mobility of the free carriers (negative for the electrons and positive for the holes); ε is the static dielectric constant of the photorefractive medium; k_b is the Boltzmann constant; T is the absolute temperature; and E_0 is the static electric field applied to the photorefractive medium in the transverse x direction. In the area of linear dielectric ($x \geq 0$) material equations take the form of a linear relation between electrical displacement and internal electric field. The material equations in both linear and nonlinear media are completed by the standard shortened wave equations for the complex slowly evolving amplitudes of the light field $A(x,z,t)$,

$$i\frac{\partial A}{\partial z} = -\frac{1}{2k_0}\frac{\partial^2 A}{\partial x^2} \quad \text{for } x \geq 0,$$

$$i\frac{\partial A}{\partial z} = -\frac{1}{2k_0}\frac{\partial^2 A}{\partial x^2} - \frac{k^2-k_0^2}{2k_0}A - \frac{k^2}{k_0 n}\delta n A \quad \text{for } x < 0, \tag{2}$$

written in the paraxial approximation. In Eqs. (2) $k_0 = \omega n_0/c$ is the wave number in the area of the linear dielectric; $k = n\omega/c$ is the wave number in the area of the photorefractive medium; n_0 is the dielectric refractive index; n is the unperturbed linear refractive index of the photorefractive medium; ω is the carrying frequency of the laser radiation; $\delta n = -(1/2)r_{\text{eff}}n^3 E_{sc}(x,z,t)$ is the nonlinear perturbation of the refractive index, arising under the influence of the internal space-charge field $E_{sc}(x,z,t)$ through the linear electro-

optic effect; r_{eff} is the effective electro-optic coefficient. Equations (1) and (2) form the closed self-consistent system that enables one to describe the interdependence of the spatial distribution of the light intensity in the incident beam and internal space-charge field E_{sc} in the area of a nonlinear photorefractive medium or free diffraction in the area of a linear dielectric.

Further we consider material equations (1) in the steady state, when $\partial/\partial t \rightarrow 0$. Under typical for the photorefractive crystals assumption $n_a \gg n_e$, the system (1) can be resolved with respect to the internal space-charge field $E_{\text{sc}}(x,z,t)$, which in the first order (see for derivation [18,19]) is given by expression $E_{\text{sc}} = [E_0 I_{\text{dark}} + (k_b T/e)(\partial I/\partial x)](I + I_{\text{dark}})^{-1}$. Substituting an internal field in such form into the shortened wave equations (2) and performing the standard normalization procedure one can finally obtain the following evolution equations for the normalized complex amplitude of the light field $q(\eta,\xi)$ in the areas of linear dielectric ($\eta \geq 0$) and nonlinear photorefractive medium ($\eta < 0$):

$$i\frac{\partial q}{\partial \xi} = -\frac{1}{2}\frac{\partial^2 q}{\partial \eta^2} \quad \text{for} \quad \eta \geq 0, \tag{3a}$$

$$i\frac{\partial q}{\partial \xi} = -\frac{1}{2}\frac{\partial^2 q}{\partial \eta^2} - pq - \frac{q|q|^2}{1+S|q|^2} + \mu\frac{q}{1+S|q|^2}\frac{\partial|q|^2}{\partial \eta}$$

$$\text{for} \quad \eta < 0. \tag{3b}$$

Here $q(\eta,\xi) = (kL_{\text{dif}}/k_0 L_{\text{ref}})^{1/2}A(\eta,\xi)I_{\text{dark}}^{-1/2}$ is the dimensionless amplitude of the light field; $A(\eta,\xi)$ is the slowly varying envelope of the light field; $\eta = x/x_0$ is the normalized transverse coordinate; x_0 is the characteristic transverse scale (for example, the width of the input laser beam); $\xi = z/L_{\text{dif}}$ is the normalized longitudinal coordinate; $L_{\text{dif}} = k_0 x_0^2$ is the diffraction length in the area of linear dielectric, corresponding to the chosen transverse scale x_0; $L_{\text{ref}} = 2/(kr_{\text{eff}}n^2 E_0)$ is the nonlinear refraction length; the saturation parameter $S = k_0 L_{\text{ref}}/kL_{\text{dif}}$ describes the relative strength of the local drift component of the nonlinear response; parameter $\mu = k_b T/(x_0 e E_0)$ describes the relative strength of the nonlocal diffusion component of the nonlinear response; guiding parameter $p = (1/2)(k^2 - k_0^2)x_0^2 - S^{-1}$ describes the waveguiding properties of the boundary and can take both positive and negative signs (corresponding to the two different types of reflection from the interface in linear approximation: ''internal'' reflection when the refractive index of photorefractive materials exceeds that of the dielectric and ''external'' reflection when the dielectric have higher refractive index than photorefractive material).

The first term in the right-hand side of Eq. (3b) describes the diffraction spreading of the light beam; the second one accounts for the beam refraction in the presence of the guiding structure (boundary); the third one describes the self-focusing of the beam due to the local drift component of nonlinear response and, finally, the last term accounts for the effects of self-bending of the beam in the propagation process due to the stimulated transfer of the energy from the lower-frequency spatial components into the high-frequency components. Equations (3) should be completed with conditions of continuity of both function q and $\partial q/\partial \eta$ at the point $\eta = 0$ that corresponds, respectively, to the continuity of the tangential component of the electric field and normal component of the magnetic field at the boundary. There are several regimes of propagation of the laser beam near the boundary [15]. If the laser beam is launched into the photorefractive medium far from the boundary, it self-bends toward the boundary in the process of propagation, thus acquiring a definite incidence angle when it approaches the boundary. If the incidence angle exceeds the total internal reflection angle, the beam experience total internal reflection that results in periodic near-boundary oscillations. If the incidence angle is less then the total internal reflection angle, the beam can be partially refracted into the linear dielectric medium and the experience diffraction spreading. Formation of the stationary surface waves corresponds in this case to the launching of the beam close to the boundary and the exact balance between the competing processes of reflection from a less optically dense linear dielectric and beam self-bending toward the boundary. Equations analogous to Eqs. (3) were used in Ref. [15] to derive the ordinary differential equation of the second order describing a near-boundary beam trajectory in the limit of a considerable dark irradiance level (that corresponds to $S \rightarrow 0$).

Typical experimentally achievable values of parameters S and μ for the SnBaNb crystal and beams of the He-Ne laser with intensities of the order of μW/cm^2 at a wavelength $\lambda = 633$ nm, for the input beam radius $x_0 \sim 50\ \mu$m, the effective electro-optic coefficient $r_{\text{eff}} = 2.5 \times 10^{-10}$ m/V, the unperturbed refractive index $n = 2.35$, the crystal temperature $T = 300$ K, and an external electric field $E_0 = 6 \times 10^3$ V/m is of the order of $S \sim 1$ and $\mu \sim 0.1$. Guiding parameter p varies within rather wide frames depending on the difference between the refractive index n_0 of the linear dielectric and unperturbed refractive index n of nonlinear photorefractive medium.

In this paper we concentrate solely on the investigation of specific features of the stationary surface waves existing at the boundary, we numerically calculate profiles of the surface waves of the different orders and corresponding dispersion diagrams, and both numerically and analytically consider stability of the obtained solutions with respect to small perturbations of the input profiles.

III. STATIONARY PROFILES OF THE SURFACE WAVES

To find stationary localized solutions of the system of equations (3), describing profiles of the surface waves we write the field of the wave in the form $q(\eta,\xi) = \rho(\eta)\exp(ib\xi)$, where a purely real wave shape $\rho(\eta) \rightarrow 0$, as $\eta \rightarrow \pm\infty$, and b being the real propagation constant. Substituting a wave field in such form into the shortened wave equations (3) we obtain the ordinary differential equations of the second order regarding $\rho(\eta)$,

$$\frac{d^2\rho}{d\eta^2} = 2b\rho \quad \text{for} \quad \eta \geq 0, \tag{4a}$$

$$\frac{d^2\rho}{d\eta^2} = 2(b-p)\rho - \frac{2\rho^3}{1+S\rho^2} + \frac{4\mu\rho^2}{1+S\rho^2}\frac{d\rho}{d\eta} \quad \text{for} \ \eta < 0,$$

$$(4b)$$

where both ρ and $d\rho/d\eta$ should match the continuity conditions at the boundary point $\eta=0$. Due to the saturable character of the photorefractive nonlinear response and the presence of the nonlocal diffusion component the system of equations (4) cannot be solved analytically and numerical integration is necessary. To find the stationary solutions of system (4) we use the shooting method that enables one to transform a two-point boundary problem into a Caushy problem. The starting conditions were chosen using the fact that in the area of linear dielectric the first of Eqs. (4) admits exact analytical solution $\rho(\eta) = m \exp[-(2b)^{1/2}\eta]$, where m is the free parameter describing the strength of the nonlinear effects. Varying the values of parameters b, S, μ, and m we obtain various profiles of the surface waves available at the boundary between the linear dielectric and photorefractive medium. Note that the saturation parameter S is inversely proportional to the static electric field E_0 applied to the photorefractive medium. The diffusion parameter μ is also inversely proportional to the static electric field E_0 and increases with a decrease of the input beam radius. Parameter m in fact defines the amplitude of the nonlinear surface wave and consequently its propagation constant b.

It is rather convenient to classify all possible types of solutions of the system (4) using quite general treatment, based on the direct analogy of Eqs. (4) for the envelope of the surface modes and the equation describing the motion of the mechanical particle in the potential well with nonlinear dissipation, where the wave amplitude ρ is equivalent to the particle position (or shift from the equilibrium point), and transverse coordinate η is equivalent to time. One can see that in the area of the nonlinear photorefractive medium ($\eta < 0$) Eq. (4b) can be rewritten in the following form:

$$\frac{d}{d\eta}(U+T) = \frac{4\mu\rho^2}{1+S\rho^2}\left(\frac{d\rho}{d\eta}\right)^2,$$

$$U = \left(\frac{1}{S} - b + p\right)\rho^2 - \frac{1}{S^2}\ln(1+S\rho^2), \quad (5)$$

$$T = \frac{1}{2}\left(\frac{d\rho}{d\eta}\right)^2,$$

where U and T are, respectively, potential and kinetic energies of the particle with unity mass, and the right-hand side of the first of Eqs. (5) describes the force of nonlinear friction which is proportional to the square of the particle speed $d\rho/d\eta$ and parameter μ describing the strength of diffusion effects. The typical profiles of the potential $U(\rho)$ for the various values of propagation constant b, guiding parameter p, and saturation parameter S are presented in Fig. 1. Note that the potential $U(\rho)$ is symmetric with respect to the point $\rho=0$, so in the figure we present only the right part of the potential corresponding to the positive values of ρ. One can see that the profile of the potential well U experiences quali-
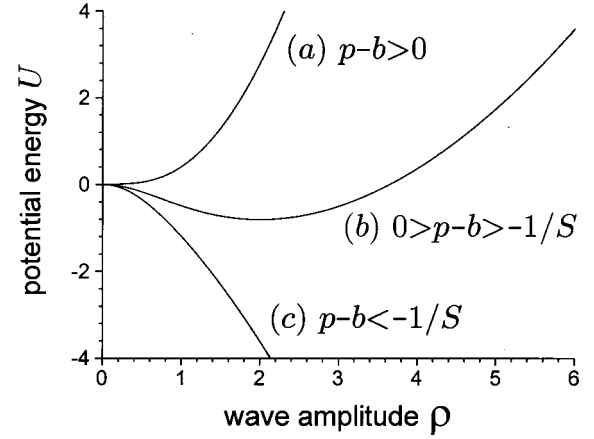

FIG. 1. Typical profiles of the potential $U(\rho)$ for the different relations between propagation constant b, guiding parameter p, and parameter S. All quantities are plotted in arbitrary dimensionless units.

tative transformations with a change of the sign of the propagation constant b, which in turn affects the character of the possible particle motions described by Eqs. (5), and, finally, profiles of corresponding surface modes.

In the case of the positive difference between the guiding parameter and the propagation constant $p-b>0$ potential U has one stable stationary point $\rho=0$ (curve a in Fig. 1), i.e., this point is a local minimum of potential U so $dU(\rho=0)/d\rho=0$ and $d^2U(\rho=0)/d\rho^2>0$ (note that the local maximum corresponds to the negative second derivative $d^2U/d\rho^2$). In this case a mechanical particle with nonzero initial energy $U+T$ describing the corresponding surface mode will experience decaying oscillations (with a change of η in the "negative" direction from 0 to $-\infty$), moving periodically from the right wing of the potential well (positive ρ) to the left wing (negative ρ), and consequently losing its energy due to the influence of nonlinear friction. As $\eta \to -\infty$ a particle asymptotically approaches the stable stationary point $\rho=0$. This type of particle motion corresponds to the well-known *delocalized* surface waves [12] having long oscillating tails in the volume of the photorefractive medium. Typical profiles of such waves are shown in Fig. 2. Careful numerical integration of Eqs. (4) and an analysis of the asymptotic expression $\rho(\eta \to -\infty) \sim |\mu\eta|^{-1/2} \cos\{[2(p-b)]^{1/2}\eta\}$ for the wave shapes at $\eta \to -\infty$ show that delocalized surface waves have infinite energy due to the very slow decay of the oscillating tail. Hence, stability of the delocalized surface waves is still an open question.

In the case of the values of propagation constants b matching the relations $0>p-b>-1/S$ the potential U has two stable $\rho = \pm\{(b-p)/[1-S(b-p)]\}^{1/2}$ (local minimums) and one unstable $\rho=0$ (local maximum) stationary points (see curve b in Fig. 1). A mechanical particle with nonzero initial energy $U+T$ will be periodically transferred in this case from the right wing of the potential well into the left wing. However, the particle consequently loses its energy due to the influence of nonlinear friction and at the certain moment (at certain η) the kinetic energy becomes too small for the next transfer through the unstable stationary
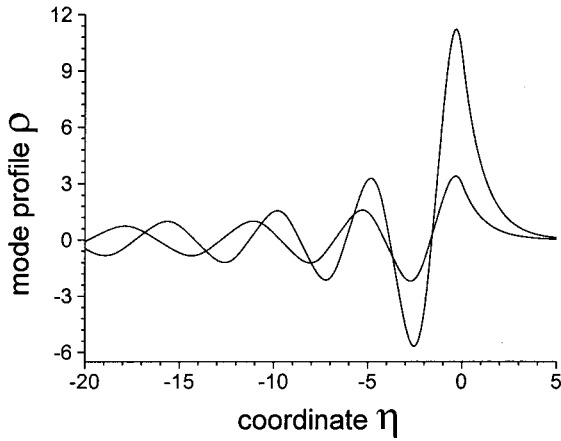
FIG. 2. Profiles of the delocalized surface waves with different amplitudes. Guiding parameter $p=0.5$, propagation constant $b=0.4$, parameters $\mu=0.2$, $S=1.0$. All quantities are plotted in arbitrary dimensionless units.

point $\rho=0$, so the particle either asymptotically approaches the unstable stationary point $\rho=0$ or remains located in one of the wings of the potential well and asymptotically approaches one of the stable stationary points $\rho=\pm\{(b-p)/[1-S(b-p)]\}^{1/2}$. The second case corresponds to the shock surface waves [36] having infinite energy and nonzero asymptotics at $\eta\rightarrow-\infty$. Typical profiles of the shock surface waves of the first three orders are presented in Fig. 3 (further we define the order of the surface wave as a number of wave zeros plus one). One can see from Fig. 3 that at the $\eta\rightarrow-\infty$ surface shock waves have the form of decaying oscillations superimposed at the constant background where height is given by expressions for position of the stable stationary point. The amplitude of oscillations and decay rate increases with an increase of the value of the diffusion parameter μ. Note that the shock waves presented above are highly unstable in the diffusion medium since they have zero harmonic in the spatial spectrum and are affected by modulation instability.
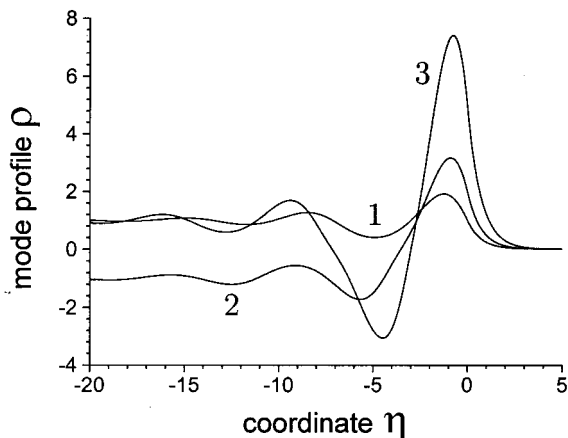

FIG. 3. Profiles of the shock surface waves of the first three orders. Guiding parameter $p=0.5$, propagation constant $b=1.0$, parameters $\mu=0.2$, $S=1.0$. All quantities are plotted in arbitrary dimensionless units.
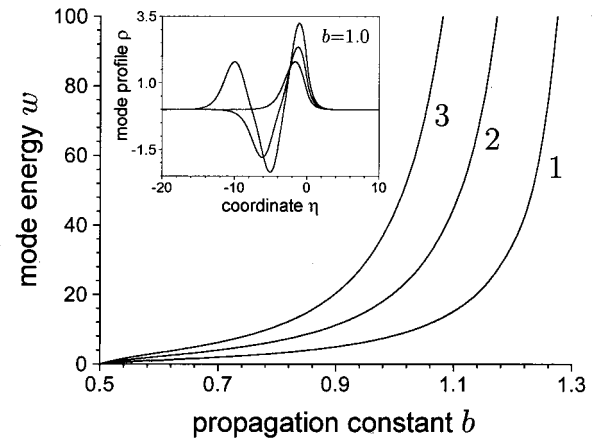

FIG. 4. Dependencies of the surface mode energy w on the propagation constant b for the first three surface modes for positive guiding parameter $p=0.5$. The inset shows profiles of the surface modes of the first three orders for $b=1.0$. Parameters $\mu=0.1$, $S=1.0$. All quantities are plotted in arbitrary dimensionless units.

Most interesting from a practical point of view is the case when a particle describing the profile of surface waves asymptotically approaches an unstable stationary point $\rho=0$ (we still consider the interval $0>p-b>-1/S$). This situation corresponds to the formation of the *localized* surface waves. There are two conventionally distinct types of the localized surface waves corresponding to the negative and positive values of the guiding parameter p. Typical profiles of the localized surface waves for a positive value of p are presented in the inset in Fig. 4, whereas profiles for a negative value of p are presented in Fig. 5. The main difference between these two regimes is that the surface wave corresponding to negative p can have a long slowly decaying tail in linear medium so the considerable part of the energy of the surface wave can be concentrated in the area of the dielectric, whereas for positive p the part of the energy concentrated in the nonlinear photorefractive medium is always higher than that in the dielectric (compare Figs. 4 and 5). This is a consequence of the fact that for negative p relation $b-p>0$ is matched for all $b\geqslant 0$, thus providing unlimited growth of mode energy

$$w=\int_{-\infty}^{\infty}\rho^2(\eta)d\eta \tag{6}$$

as $b\rightarrow 0$ according to the exact expression for the surface wave shape in the area of linear dielectric $\rho(\eta)=m\exp[-(2b)^{1/2}\eta]$ that follows from Eq. (4a). Dispersion diagrams (dependence of the mode energy w on the value of the propagation constant b) for the first three surface modes and negative guiding parameter p are shown in Fig. 5. As for the case of a boundary between the dielectric and the Kerr medium [2] dependence of energy on the propagation constant is nonmonotonic. For the case of positive values of the p mode energy w goes to zero as $b\rightarrow p$ and monotonically increases with an increase of the propagation constant b (see Fig. 4 with dispersion diagrams for the first three surface
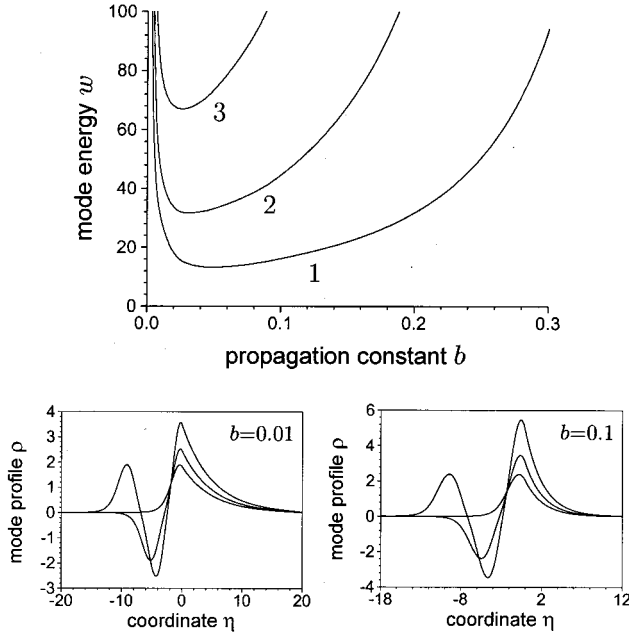
FIG. 5. Dependencies of the surface mode energy w on the propagation constant b for the first three surface modes for negative guiding parameter $p = -0.5$. Subfigures show profiles of the surface modes of the first three orders for propagation constant values $b = 0.01$ and $b = 0.1$ corresponding to the different signs of dw/db. Parameters $\mu = 0.1$, $S = 1.0$. All quantities are plotted in arbitrary dimensionless units.

modes). It will be shown further that this characteristic behavior of dispersion curves in the presence of a nonlocal diffusion component of photorefractive response can be associated with linear stability or instability of corresponding surface modes just as for the case of the local Kerr material. Note the following characteristic feature of the profiles of localized surface waves: starting from the values of $n = 2$ the profiles of the $(n + 1)$-order wave without the first closest to the boundary period coincide with the profiles of the n-order wave without the first half-period. With an increase of mode energy the profile of the surface mode becomes more and more asymmetric. This is due to the influence of the diffusion component of nonlinear response. The position of the intensity maximum shifts toward the boundary because for the compensation of the influence of self-bending effects (which is approximately proportional to the fourth power of the wave amplitude) it is necessary to increase the strength of the boundary effects. As propagation constant b approaches the approximate value $p + 1/S$ the mode energy goes to infinity—the mode amplitude in this case increases whereas the characteristic transverse extent decreases. In the limit of high amplitudes Eq. (4b) can be linearized and admits the following analytical solution $\rho(\eta) = m \exp(2\mu S^{-1}\eta) \times \cos[(2S^{-1} - 2b + 2p - 4\mu^2 S^{-2})^{1/2}\eta]$, giving the more accurate than $p + 1/S$ estimate of the upper limiting value of the propagation constant b at which localized surface waves are still possible,

$$b = p + \frac{1}{S} - \frac{2\mu^2}{S^2}. \tag{7}$$

As for the usual saturable optical medium an increase of the saturation parameter S at fixed μ and p results in the flattening of the corresponding profiles of the surface modes, i.e., in an increase of the characteristic transverse extent of the modes (full width at half maximum) with the same energies. Stability of the localized surface modes will be considered in the next section.

Finally, returning to the example with the mechanical particle we consider the last case when the propagation constant $b > p + 1/S$. In this case potential U has the only unstable stationary point $\rho = 0$ (see curve c in Fig. 1). In this case the finite motion is impossible except for the trivial case of zero initial energy $U + T$. A particle with nonzero $U + T$ will go away from $\rho = 0$, which corresponds to infinitely increasing oscillations of the light field so it is useless to speak about surface waves in this case.

IV. STABILITY OF THE LOCALIZED SURFACE WAVES

To investigate the stability of the localized surface waves at the boundary between the linear dielectric and the photorefractive medium with drift and diffusion nonlinearity we use the well-known linear stability analysis which is valid at the initial stage of perturbation development. Note that an earlier linearization technique was used mostly for the analysis of the stability of optical solitons in local medium, where nonlinear perturbation of the refractive index depends solely on the light intensity and does not contain derivatives of light intensity on transverse coordinates [25–34]. In our case, however, the presence of a nonlocal diffusion component of the nonlinear response strongly affects dispersion diagrams (profiles of corresponding surface waves) and also breaks the assumptions that are usually used for the derivation of widespread VK criterion provided that this criterion (if it is applicable in nonlocal materials) calls for the separate justification. We will search for the solutions of Eqs. (3) that describe the propagation of the surface waves with perturbed input profiles of the following form:

$$q(\eta, \xi) = [\rho(\eta) + u(\eta, \xi) + iv(\eta, \xi)]\exp(ib\xi), \tag{8}$$

where, as earlier, $\rho(\eta)$ is the real stationary shape of the surface wave; functions $u(\eta, \xi)$ and $v(\eta, \xi)$ are, respectively, the real and imaginary parts of the small $(u, v \ll \rho)$ perturbation. Assumption of the small comparative amplitude of perturbation, which is a quite general condition for the fundamental surface waves with no nodes, is rather restrictive, however, for the surface modes of higher orders. Thus the small perturbation matching this condition should be zero at the points where the corresponding surface mode goes to zero, so a rather narrow class of perturbations can be considered with the aid of the linearization technique for higher-order modes and for proper analysis it is necessary to use nonlinearized equations (3). Hence, we now concentrate solely on the investigation of the stability of the fundamental modes. Substitution of expression (8) into shortened wave equations (3), subsequent linearization, and the derivation of the real and imaginary parts yields the following system of linear equations:

$$\frac{\partial u}{\partial \xi} = -\mathcal{L}v,$$

$$\frac{\partial v}{\partial \xi} = \mathcal{R}u,$$

$$(9)$$

where linear operators $\mathcal{L}$ and $\mathcal{R}$, depending on the transverse coordinate η, have the following form in the area of nonlinear photorefractive medium ($\eta < 0$):

$$\mathcal{L} = \frac{1}{2}\frac{d^2}{d\eta^2} - b + p + \frac{\rho^2}{1 + S\rho^2} - \frac{2\mu\rho}{1 + S\rho^2}\frac{d\rho}{d\eta},$$

$$\mathcal{R} = \mathcal{L} + \frac{2\rho^2}{(1 + S\rho^2)^2} + \frac{4\mu S\rho^3}{(1 + S\rho^2)^2}\frac{d\rho}{d\eta} - \frac{2\mu\rho}{1 + S\rho^2}\frac{d\rho}{d\eta}$$

$$- \frac{2\mu\rho^2}{1 + S\rho^2}\frac{d}{d\eta}.$$

$$(10)$$

Note that in the area of linear dielectric ($\eta \geq 0$) operators $\mathcal{L} = \mathcal{R} = (1/2)(d^2/d\eta^2) - b$. One can see from the form of expressions (10) that unlike for the medium with local nonlinear response the linear operator $\mathcal{R}$ is not self-adjoint in the medium with nonlocal diffusion component of nonlinear response due to the presence of the last term, containing the derivative of the first order on coordinate η, whereas linear operator $\mathcal{L}$ is still self-adjoint. The last circumstance prevents an attempt to perform the standard procedure of derivation of the VK stability criterion, since eigenvalues of the combined operators $\mathcal{L}\mathcal{R}$ and $\mathcal{R}\mathcal{L}$ may now be complex (this will indicate the presence of perturbations experiencing, besides exponential growth, simultaneous harmonic oscillations along the ξ axis), but not purely real (such a facts corresponds to the existence of either exponentially growing perturbations or perturbations experiencing harmonic oscillations) as it was in the medium with local nonlinear response. The following properties of the operators $\mathcal{L}$ and $\mathcal{R}$ are

$$\mathcal{L}\rho = 0,$$ (11a)

$$\mathcal{R}\frac{d\rho}{d\eta} = 0,$$ (11b)

$$\mathcal{R}\frac{d\rho}{db} = \rho,$$ (11c)

will be used further and can be easily verified by direct substitution of ρ, $d\rho/d\eta$, and $d\rho/db$ into expressions for operators (10).

We will search for solutions of system (9) in the form of decomposition on all possible perturbations with various increments

$$u(\eta,\xi) = \text{Re}\left(\sum_{\delta} C_\delta u_\delta(\eta)\exp(\delta\xi)\right),$$

$$v(\eta,\xi) = \text{Re}\left(\sum_{\delta} C_\delta v_\delta(\eta)\exp(\delta\xi)\right),$$

$$(12)$$

where δ is the complex increment (growth rate) of perturbation, C_δ is the arbitrary constants, and u_δ and v_δ are the complex input profiles of the perturbation. Under the substitution of series (12) into the linear system (9) and the equation of terms with the same exponential coefficients $\exp(\delta\xi)$, one can obtain the following final system of linear equations with real linear operators $\mathcal{L}$ and $\mathcal{R}$:

$$\delta u_\delta = -\mathcal{L}v_\delta,$$

$$\delta v_\delta = \mathcal{R}u_\delta.$$

$$(13)$$

First of all we solved system (13) numerically, taking into account the vanishing asymptotics of the perturbation at $\eta \to \pm\infty$ and the continuity conditions at the interface between the dielectric and photorefractive medium. We were mainly interested here in the calculation of the dependencies of the real and imaginary parts of the increment δ as functions of propagation constant b. Numerical integration shows that for positive values of the guiding parameter p system Eqs. (13) allow only solutions corresponding to the purely imaginary increments δ, so perturbed surface waves conserve the input structure upon propagation whereas arbitrary small perturbation will experience harmonic oscillations along the longitudinal ξ axis. Dependence of the imaginary part of the increment δ on the propagation constant b for the positive guiding parameter p is presented in Fig. 6(a). Note that the given value of the propagation constant b can correspond to several perturbation modes with different increments δ [several solutions of the system (13)]. As $b \to p + S^{-1} - 2\mu^2 S^{-2}$ the number of possible perturbation modes infinitely increases [Fig. 6(a) shows dependencies Im $\delta(b)$ only for the first three perturbation modes] and corresponding values of increments tend to zero. Curves corresponding to the different perturbation modes branch off the strait line Im $\delta = b - p$. Figures 6(c)–6(e) show normalized perturbation profiles (u and v components) for the propagation constant value $b = 1.4$ [at this value of propagation constant there exist only three solutions of system (13)]. Since for positive values of p the increment δ is purely imaginary it follows from the system (13) that at purely real component v component u must be purely imaginary. One can see that despite the fact that the corresponding fundamental surface wave has on nodes [Fig. 6(b)] the lowest order perturbation mode has one node [Fig. 6(c)], the perturbation mode of the next order has two nodes [Fig. 6(d)], etc. With an increase of the perturbation order profiles of u and v components practically coincide [Fig. 6(e)]. Note that for the surface modes of the highest orders calculations in the frames of the model (8)–(13) also indicate the absence of exponentially growing perturbations for positive p; however, this fact is not sufficient to prove the stability due to the strong restrictions imposed on the perturbation profile by conditions $u, v \ll \rho$.

The picture, however, qualitatively changes for the negative values of guiding parameter p. In this case system (13) allows solutions corresponding to the purely real increment δ in the certain interval of the propagation constant values [see the inset in the Fig. 7(a)], i.e., exponentially growing perturbations were found. Outside this interval only solutions cor-
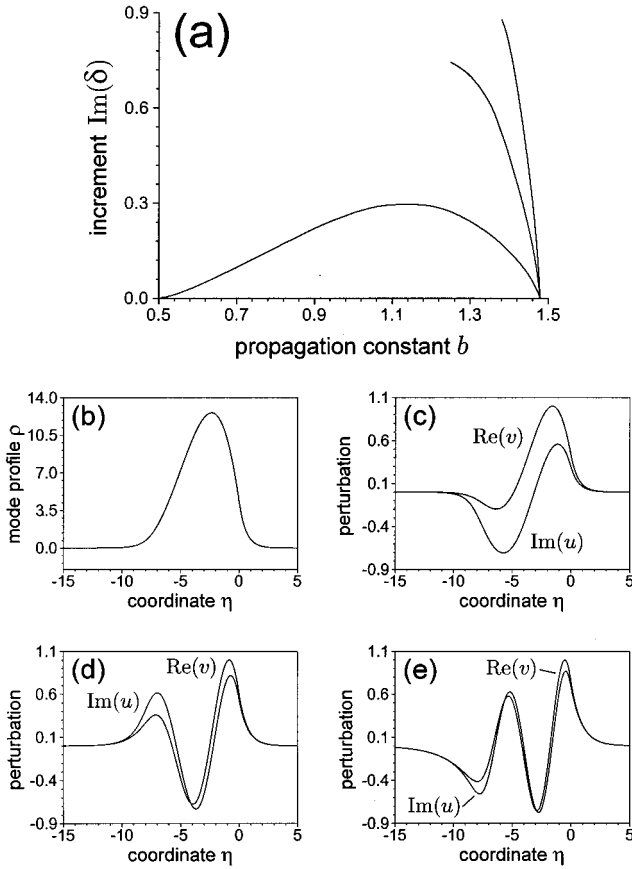
FIG. 6. (a) shows the typical dependence of the imaginary part of increment δ on the propagation constant b for the fundamental surface wave and positive guiding parameter p. (b) shows the profile of the stable fundamental surface wave for $b=1.4$ whereas (c)–(e) show profiles of the corresponding normalized perturbation components u and v. Guiding parameter $p=0.5$, parameters $\mu=0.1$, $S=1.0$. All quantities are plotted in arbitrary dimensionless units.

FIG. 7. (a) shows the typical dependence of the imaginary part of increment δ on the propagation constant b for the fundamental surface wave and negative guiding parameter p. The inset in (a) shows the dependence of the real part of increment δ on the propagation constant b. (b) shows a profile of the unstable fundamental surface wave for $b=0.03$ whereas (c) shows profiles of the corresponding normalized perturbation components. (d) shows a profile of the stable fundamental surface wave for $b=0.72$ whereas (e)–(g) show profiles of the corresponding normalized perturbation components. Guiding parameter $p=-0.2$, parameters $\mu=0.1$, $S=1.0$. All quantities are plotted in arbitrary dimensionless units.

responding to the purely imaginary increments exist [Fig. 7(a)]. Thus in the case of the medium with a diffusion component of nonlinear response (as for the case of the dielectric–Kerr medium boundary [2]), at negative values of guiding parameter p we still did not find mixed solutions corresponding to increments with simultaneously nonzero real and imaginary parts, i.e., real and imaginary parts of the increment goes to zero at the same point b_0. One can clearly see it if we compare dependencies Im $\delta(b)$ and Re $\delta(b)$ presented in Fig. 7(a). Typical examples of surface wave and profiles of perturbation that correspond to the purely real value of increment δ are presented in Figs. 7(b) and 7(c). As one can see the unstable surface mode has a long slowly decaying tail in the linear medium [Fig. 7(b)]. Profiles of the surface mode [Fig. 7(d)] and perturbation modes [Figs. 7(e)–7(g)] corresponding to the purely imaginary increments δ are analogous to that presented for the case of positive guiding parameter p. One can see that system (13) has no localized solutions in the certain region of propagation constants (part of the curve showing an imaginary increment for the lowest
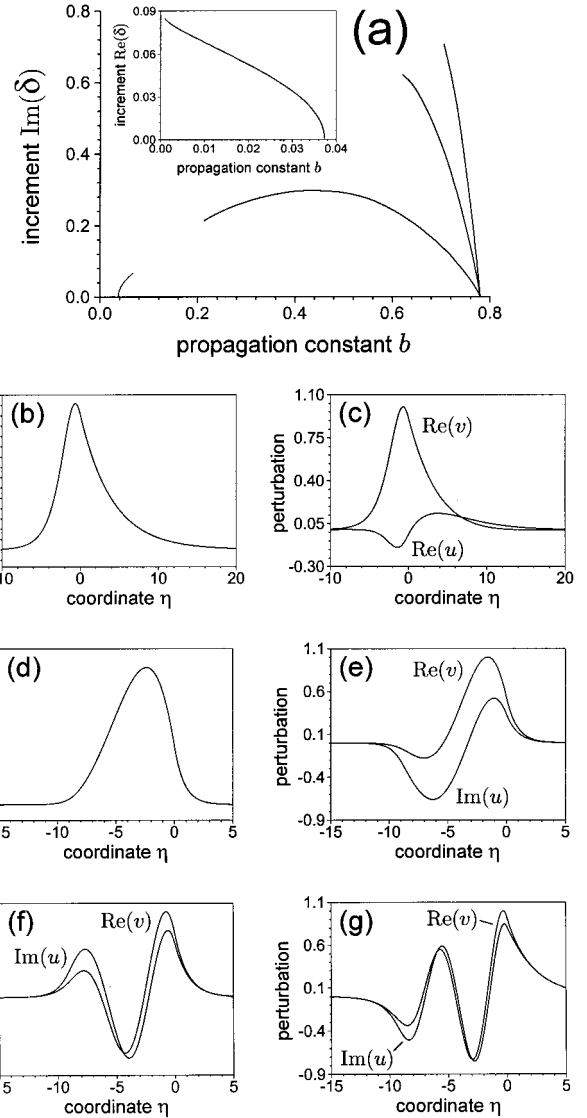
order perturbation mode in this region is cut off by the strait line Im $\delta=b$ that divides the areas of harmonic (along η) and exponentially decaying at $\eta\to\pm\infty$ perturbations). Direct comparison of the results of integration of system (13) presented in the Figs. 6 and 7 with corresponding dispersion diagrams for positive and negative values of guiding parameter p (Figs. 4 and 5) shows that as for the case of the dielectric–Kerr medium boundary fundamental surface waves at the boundary dielectric–photorefractive medium

with drift and diffusion nonlinearity are stable if $dw/db > 0$ and unstable if $dw/db < 0$.

The latter conclusion that point b_0 where $dw/db = 0$ derives the areas of existence of stable and unstable modes can also be proved analytically if one take into account that in this point b_0 both Im δ and Re δ goes to zero. When $\delta = 0$ the system (13) transforms into two independent linear equations for the perturbation components:

$$\mathcal{L}v = 0,$$
$$\mathcal{R}u = 0. \tag{14}$$

In the volume of the photorefractive medium (at $\eta \rightarrow -\infty$) amplitude of the localized surface wave quickly decreases. When amplitude ρ is small enough, nonlinear terms in Eq. (4b) describing the wave profile can be neglected, provided that asymptotic expressions for the surface wave profile and its transverse derivative are given by $\rho \sim d\rho/d\eta \sim \exp[(2b - 2p)^{1/2}\eta]$ as $\eta \rightarrow -\infty$. In the area of linear dielectric ($\eta \geqslant 0$) the first of Eqs. (4) have exact analytical solution $\rho(\eta) = \rho_0 \exp[-(2b)^{1/2}\eta]$ where $\rho_0 = \rho(\eta = 0)$. Corresponding asymptotic expressions for the linear operators $\mathcal{L}$ and $\mathcal{R}$ have the form [see formula (10)]:

$$\mathcal{L}|_{\eta \rightarrow -\infty} \approx \mathcal{R}|_{\eta \rightarrow -\infty} \approx \frac{1}{2}\frac{d^2}{d\eta^2} + p - b,$$

$$\mathcal{L}|_{\eta \geqslant 0} = \mathcal{R}|_{n \geqslant 0} = \frac{1}{2}\frac{d^2}{d\eta^2} - b. \tag{15}$$

As far as we consider localized perturbations, substitution of the expressions (15) for the operators into Eqs. (14) leads to the following asymptotic expressions for the perturbation profiles: $u \sim v \sim \exp[(2b - 2p)^{1/2}\eta]$ as $\eta \rightarrow -\infty$, and $u = u_0 \exp[-(2b)^{1/2}\eta]$, $v = v_0 \exp[-(2b)^{1/2}\eta]$ for $\eta \geqslant 0$, where $u_0 = u(\eta = 0)$ and $v_0 = v(\eta = 0)$. Comparing linear equations (14) with Eqs. (11a) and (11b), and taking into account the coincidence of the asymptotic expressions for u, v, ρ, and $d\rho/d\eta$, one obtains that at zero increment value the perturbation component v is proportional to ρ and component u is proportional to $d\rho/d\eta$ everywhere in the dielectric and photorefractive medium if continuity conditions are matched.

Further we will show that for continuity conditions matching it is necessary to have zero coefficient of proportionality between u and $d\rho/d\eta$, i.e., the only solution of the linear equation $\mathcal{R}u = 0$ that matches to the continuity of the function u and its first derivative $du/d\eta$ at the boundary point $\eta = 0$ is trivial solution $u = 0$. Since in the area of dielectric $\rho = \rho_0 \exp[-(2b)^{1/2}\eta]$ and ρ, $d\rho/d\eta$ match the continuity conditions, one can write that $d\rho(\eta = 0)/d\eta = -(2b)^{1/2}\rho_0$ and $d^2\rho(\eta = 0)/d\eta^2 = 2b\rho_0$ and substitute this expressions into Eq. (4b) (supposing also continuity of $d^2\rho/d\eta^2$). This gives the following value of amplitude ρ_0:

$$\rho_0^2 = -\frac{p}{1 + Sp + 2^{3/2}\mu b^{1/2}}. \tag{16}$$

For the positive guiding parameter p the right part of expression (16) is negative whereas the left one is assumed to be positive. It means that the second derivative $d^2\rho/d\eta^2$ of the surface wave profile is not continuous at the boundary (at $\eta = 0$) whereas ρ and $d\rho/d\eta$ are continuous.

For negative p substitution of the amplitude (16) and the corresponding derivative $d\rho(\eta = 0)/d\eta$ into expressions (5) for potential U and kinetic T energies results in negative total energy $U + T$ at which localized surface waves are impossible (see Fig. 1), and hence one again obtains that the second derivative $d^2\rho/d\eta^2$ is not continuous. This in turn shows that the transverse derivative of the perturbation component $du/d\eta$ is not continuous at the boundary if $u \sim d\rho/d\eta$ with a nonzero coefficient of proportionality, and hence the only solution of the linear equation $\mathcal{R}u = 0$ matching the continuity conditions is the trivial solution $u = 0$.

Let us consider the small shift ε of the propagation constant b from the ''stationary'' value b_0 corresponding to the zero increment $\delta = 0$ toward the area of propagation constant values corresponding to the unstable modes. As it was shown above, at $\delta = 0$ perturbation components $u = 0$ and $v \sim \rho$. This allows us to write expressions for increment and perturbation profiles corresponding to new b in the following form:

$$u(\eta) = u_m(\eta)\varepsilon^k,$$
$$v(\eta) = \alpha\rho(\eta)|_{b=b_0} + v_m(\eta)\varepsilon^l, \tag{17}$$
$$\delta \sim \varepsilon^n,$$

where $u_m(\eta)$ and $v_m(\eta)$ are the arbitrary functions of the transverse coordinate describing the modification of the perturbation profile; α is the arbitrary coefficient. Linear operators (10) also change with a change of b and can be expressed in the form of expansions in a Fourier series,

$$\mathcal{L} = \mathcal{L}|_{b=b_0} + \varepsilon\frac{\partial\mathcal{L}}{\partial b}\bigg|_{b=b_0} + \frac{1}{2}\varepsilon^2\frac{\partial^2\mathcal{L}}{\partial b^2}\bigg|_{b=b_0} + \cdots,$$
$$\mathcal{R} = \mathcal{R}|_{b=b_0} + \varepsilon\frac{\partial\mathcal{R}}{\partial b}\bigg|_{b=b_0} + \frac{1}{2}\varepsilon^2\frac{\partial^2\mathcal{R}}{\partial b^2}\bigg|_{b=b_0} + \cdots. \tag{18}$$

Substituting perturbation profiles in the form (17) and operators (18) into system (13) and equating the terms of the lowest (with respect to the small parameter ε) orders, one can obtain that indexes $l = 1$, $k = n$ and, for instance,

$$\mathcal{R}|_{b=b_0}u_m(\eta) \sim \rho(\eta)|_{b=b_0}. \tag{19}$$

Upon comparison of expression (19) with Eq. (11c) one can conclude that the perturbation profile [see formula (17)] is proportional to

$$u \sim u_m \sim \frac{\partial\rho}{\partial b}\bigg|_{b=b_0}. \tag{20}$$

Further we will use the fact that the perturbation component u is orthogonal to the exact surface wave profile ρ, i.e.,

$$\int_{-\infty}^{\infty} u(\eta)\rho(\eta)d\eta = 0. \tag{21}$$

This expression is a consequence of the first of equations (13) and can be obtained from the latter equation after its multiplication by ρ and integration over η if ones takes into account that linear operator $\mathcal{L}$ is self-adjoint and ρ is an eigenfunction of $\mathcal{L}$. Finally substitution of expression (20) in (21) leads us to the conclusion that the energy of the fundamental surface modes at the boundary between the linear dielectric and photorefractive medium with drift and diffusion nonlinearity as a function of propagation constant b has a local extremum in the point b_0 that derives the stable and unstable modes just as in the case of the dielectric–Kerr medium boundary [1–6], i.e.,

$$\frac{\partial}{\partial b}\int_{-\infty}^{\infty} \rho^2(\eta)d\eta = 0. \tag{22}$$

Stability of the surface modes in the areas around transition point (22) for each separate configuration should be considered numerically. We note that for our case modes with $dw/db > 0$ were stable, whereas modes with $dw/db < 0$ were unstable as for the dielectric–Kerr medium boundary. Thus it is shown that VK stability criterion remains legible for the case of solitons in a photorefractive medium even in the presence of a strong diffusion component of nonlinear response (numerical integration was performed up to the values of μ of the order of unity when the influence of the diffusion component is comparable to the influence of focusing drift nonlinearity and strongly affects mode profiles).

V. CONCLUSION

In conclusion let us briefly list our main results. We consider surface waves at the interface between the linear dielectric and photorefractive medium with drift and diffusion components of nonlinear response. Using the simple analogy between the surface waves and mechanical particles situated in the certain potential and subjected to the influence of nonlinear friction we have shown that there are three types of surface waves possible at the interface under consideration: delocalized, shock, and localized surface waves. Only the last type of photorefractive surface waves have limited energy. It is shown that the influence of the diffusion component of the photorefractive crystal response results in strong asymmetry of the surface wave profiles. Typical profiles of the localized surface waves and corresponding dispersion diagrams are calculated numerically. We also both numerically and analytically investigated stability of the obtained surface modes and showed that VK stability criterion derived for local saturable or Kerr materials remains legible even in the presence of the strong nonlocal diffusion component of the PRC response.

[1] W. Tomlinson, J. Gordon, P. Smith, and A. Kaplan, Appl. Opt. **21**, 2041 (1982).

[2] N. Akhmediev, V. Korneev, and Y. Kuz'menko, Sov. Phys. JETP **61**, 62 (1985).

[3] H. Tran, J. Mitchell, N. Akhmediev, and A. Ankiewicz, Opt. Commun. **93**, 227 (1992).

[4] H. Tran and A. Ankiewicz, IEEE J. Quantum Electron. **28**, 488 (1992).

[5] W. Tomlinson, Opt. Lett. **5**, 323 (1980).

[6] N. Akhmediev, Sov. Phys. JETP **56**, 299 (1982).

[7] A. Newell and J. Moloney, *Nonlinear Optics* (Redwood City, Addison-Wesley, 1992).

[8] H. Tran, J. Nonlinear Opt. Phys. Mater. **5**, 133 (1996).

[9] J. Powell, E. Wright and J. Moloney, J. Appl. Math. Mech. **54**, 774 (1994).

[10] G. Duree, J. Shultz, G. Salamo, M. Segev, A. Yariv, B. Crosignani, P. Di Porto, E. Sharp and R. Neurgaonkar, Phys. Rev. Lett. **71**, 533 (1993).

[11] M. Iturbe-Castillo, P. Marquez-Aguilar, J. Sanchez-Mondragon, S. Stepanov, and V. Vysloukh, Appl. Phys. Lett. **64**, 408 (1994).

[12] G. Garcia-Quirino, J. Sanchez-Mondragon and S. Stepanov, Phys. Rev. A **51**, 1571 (1995).

[13] M. Cronin-Golomb, Opt. Lett. **20**, 2075 (1995).

[14] G. Garcia-Quirino, J. Sanchez-Mondragon, S. Stepanov, and V. Vysloukh, J. Opt. Soc. Am. B **13**, 2530 (1996).

[15] V. Aleshkevich, V. Vysloukh, and Y. Kartashov, Opt. Quantum Electron. (to be published).

[16] D. Christodoulides and T. Coskun, Opt. Lett. **21**, 1220 (1996).

[17] Z. Sheng, Y. Cui, N. Cheng, and Y. Wei, J. Opt. Soc. Am. B **13**, 584 (1996).

[18] D. Christodoulides and T. Coskun, J. Opt. Soc. Am. B **12**, 1628 (1995).

[19] L. Jinsong and L. Keqing, J. Opt. Soc. Am. B **16**, 550 (1999).

[20] A. Kamshilin, E. Raita, and A. Khomenko, J. Opt. Soc. Am. B **13**, 2536 (1996).

[21] A. Khomenko, A. Garcia-Weidner, and A. Kamshilin, Opt. Lett. **21**, 1014 (1996).

[22] E. Raita, A. Kamshilin, and T. Jaaskelainen, J. Opt. Soc. Am. B **15**, 2023 (1998).

[23] D. Mitchell and A. Snyder, J. Opt. Soc. Am. B **10**, 1572 (1993).

[24] N. Vakhitov and A. Kolokolov, Sov. Radiophys. **16**, 783 (1973).

[25] N. Akhmediev, A. Ankiewicz, and H. Tran, J. Opt. Soc. Am. B **10**, 230 (1993).

[26] H. Tran, J. Opt. Soc. Am. B **11**, 789 (1994).

[27] D. Mihalache, D. Mazilu, and L. Torner, Phys. Rev. Lett. **81**, 4353 (1998).

[28] Y. Chen, Phys. Rev. E **57**, 3542 (1998).

[29] D. Hutchings, J. Arnold, and D. Parker, Phys. Rev. E **58**, 6649 (1998).

[30] L. Berge, Phys. Rev. E **62**, R3071 (2000).

[31] O. Bang, Y. Kivshar, A. Buryak, A. Rossi, and S. Trillo, Phys. Rev. E **58**, 5057 (1998).

[32] D. Skryabin and W. Firth, Phys. Rev. E **60**, 1019 (1999).

[33] D. Mihalache, D. Mazilu, and L. Crasovan, Phys. Rev. E **60**, 7504 (1999).

[34] T. Alexander, Y. Kivshar, A. Buryak, and R. Sammut, Phys. Rev. E **61**, 2042 (2000).

[35] N. Kukhtarev, V. Markov, S. Odulov, M. Soskin, and V. Vinetskii, Ferroelectrics **22**, 949 (1979).

[36] V. Kutuzov, V. Petnikova, V. Shuvalov, and V. Vysloukh, J. Nonlinear Opt. Phys. Mater. **6**, 421 (1997).